ELECTROCHEMICAL RECOVERY OF MINOR CONCENTRATIONS OF GOLD FROM CYANIDE-FREE CUPRIC CHLORIDE LEACHING SOLUTIONS

Ivan Korolev [a, b], Pelin Altınkaya [a, b], Petteri Halli [b], Pyry-Mikko Hannula [b], Kirsi Yliniemi [b], Mari Lundström [b *]

[a] Outotec Research Center, P.O. Box 69, Kuparitie 10, 28101 Pori, Finland

[b] Aalto University School of Chemical Engineering, P.O. Box 16200, 00076 Aalto, Finland

* Corresponding author: mari.lundstrom@aalto.fi

Abstract

Despite of being the most common hydrometallurgical process for extraction of gold from ores and concentrates, cyanide leaching is blamed for its hazardous impact on environment and human health. These concerns have given a rise for alternative cyanide-free technologies, such as cupric chloride leaching. However, the state-of-art processes for gold recovery from chloride solutions are facing issues of high reagent consumption and poor selectivity. This article describes an innovative method for recovery of minor concentrations of gold from hydrometallurgical solutions by repetitive Electrochemical Deposition-Redox Replacement (EDRR) cycles. In contrast to conventional carbon-in-leach/resin-in-leach technologies or solvent extraction, the proposed electrochemical method does not require addition of any chemicals in the process and remarkably selective gold recovery can be achieved from concentrated cupric solution by tailoring the process parameters.

A number of electrochemical experiments was performed in order to identify the process variables affecting the Au recovery. Results indicate that so called cut-off potential and deposition time were the EDRR parameters having the strongest impact on gold recovery at fixed concentration of Cu and Au ions. The Au content in the metal deposit after 250 EDRR cycles exceeded 75% and the Au:Cu ratio has increased by a factor of 1000, from 1:340 in the solution up to 3.3:1 in the final product. X-ray photoelectron spectroscopy analysis of the cathode surface confirmed full replacement of sacrificial copper with gold. Obtained results prove that the EDRR method can be efficiently used for the recovery of trace amounts of gold from cupric chloride solutions used for cyanide-free gold leaching.

Keywords

Gold recovery, electrodeposition, redox replacement, cyclic voltammetry, cyanide-free leaching

1. Introduction

Gold cyanidation is by far the main industrial gold leaching process and it has been used for over a century in large-scale gold extraction operations all over the world (Deschênes, 2016). In spite of this, raising concerns regarding the toxicity of cyanide and its inability to efficiently leach carbonaceous and refractory ores has led to an increased interest in developing cleaner technologies for cyanide-free gold recovery (Binnemans and Jones, 2017; Bisceglie et al., 2017; Jenkin et al., 2016; Leikola et al., 2017). Actually, chlorination was applied extensively even before the introduction of the cyanidation process (Adams, 2016). In 1851, K.F. Plattner developed a process for the treatment of gold ores, which consisted of passing chlorine gas over crushed ore to produce a soluble gold chloride (Kirke Rose, 1894). However, due to high treatment cost, chlorination required high gold ore grades of about 50 g/t (Habashi, 2016). Also recently, chloride leaching of gold has been the subject of detailed studies (Baghalha, 2007; Lundström et al., 2012; Pangum and Browner, 1996; Tran et al., 2001, 1992) concerning extraction of copper and other base metals. Currently it seems to be a favorable alternative to cyanide leaching. With increasing requirements to treat more complex refractory ores and even secondary raw materials, the chloride leaching process can offer an application where other metals are extracted along with gold in more environmentally friendly manner (Forsén and Aromaa, 2013; Hasab et al., 2014; Lu et al., 2017; Nam et al., 2008; Sun et al., 2016).

The global trend in mining industry in general and in gold mining in particular is that production of metals is permanently growing but the ore grades and resource availability are steadily declining (Calvo et al., 2016; Mudd, 2007; Sverdrup and Ragnarsdóttir, 2014; Tuusjärvi et al., 2014). These issues stimulate an emerging interest for extraction of minor quantities of valuable metals from complex impure hydrometallurgical solutions, e.g. by means of electrochemical reactions (Park et al., 2015; Tanong et al., 2017; Wu et al., 2017). Specifically, the use of electrochemical methods for gold recovery is attractive as no additional chemical reagents are required and the recovery can be precisely controlled by applying favorable process conditions (Lekka et al., 2015).

Redox replacement reactions have been studied for decades for different redox pairs (Dimitrov, 2016; Hormozi Nezhad et al., 2005; Sun and Xia, 2004; Venkatraman et al., 2016). Classically, these reactions are investigated in the context of designing of functional materials: various catalysts (Benson et al., 2017; Jin et al., 2004; Machado et al., 1991), nanoparticle growth (Tian et al., 2006; Yliniemi et al., 2013; Zhang et al., 2010), formation of thin films (Al Amri et al., 2016), fuel cell applications (Brankovic et al., 2001a), etc. Brankovic *et al.* (2001b) introduced a two-step method of forming thin films by surface-limited redox replacement (SLRR) which utilizes underpotential deposition of Cu (less noble metal, also called sacrificial metal) coupled with a subsequent galvanic displacement of that layer by

a more noble metal of interest such as Ag, Pt or Pd from another solution. This method was further developed by using a flow cell or one-cell configuration (Mitchell et al., 2012; Thambidurai et al., 2009). Sheridan *et al.* (2013) demonstrated that chloride complexation improves formation of Pd thin films using SLRR of underpotentially deposited copper. Viyannalage *et al.* (2007) studied the deposition of Cu by SLRR of Pb adlayer in one-cell configuration and concluded that the key to successful monolayer growth is the proper ratio of sacrificial metal ions to replacing metal ions in the solution, which for his study was 33:1. However, in gold chloride leaching processes, the composition of the hydrometallurgical process solution is not adjusted to achieve favorable ratio between metals for electrochemical recovery, but it contains inherently high concentration of cupric ions (oxidant) with only minor gold concentration in solution (Ahtiainen and Lundström, 2016; Leppinen et al., 2005; Lundström et al., 2014; Miettinen et al., 2013). This brings along a new challenge, as high base metal concentrations and impurity dissolution may hinder the best available gold recovery technology by carbon-in-leach (CIL) or resin-in-leach (RIL) due to co-adsorption.

This paper provides a novel clean technology approach for gold recovery from cyanide-free solutions with only minor gold concentration. Recently, Halli *et al.* (2017) described a method of silver recovery from zinc-containing solutions by means of cyclic electrodeposition-redox replacement (EDRR). EDRR resembles SLRR deposition method performed in a single electrolyte bath (Fayette et al., 2011), but the goal in this study is to form rich layer of pure gold deposit rather than functional or nanostructured layer. To the best of authors' knowledge, there are no reports of utilizing SLRR type methods or repetitive electrochemical atomic layer deposition cycles for the recovery of gold from any hydrometallurgical solutions. The results presented in this paper introduce a novel method for the extraction of gold from cupric chloride solutions, typical for emerging cyanide-free gold leaching processes, e.g. Nippon Mining & Metals (Toraiwa and Abe, 2000), PLASTOL (Ferron et al., 2003), Intec (Moyes et al., 2005), Nichromet (Lemieux et al., 2013), Outotec Gold Chloride process (Miettinen et al., 2013), by EDRR. This method can offer an exceptional selectivity for gold recovery directly from leaching solutions without any chemical addition into the process.

2. Experimental

2.1. Materials

Four synthetic electrolyte solutions simulating gold chloride leaching solutions were prepared by dissolving in deionized water NaCl (≥99.0%, Merck), $CuCl_2 \cdot 2H_2O$ (98% pure, Acros Organics) and Gold Atomic Absorption Standard AA22H-1 (1000 µg/mL Au, AccuStandard) in quantities required to obtain concentrations as quoted in Table 1. The experiments were performed in a three-electrode cell (50

cm^3) with parallel plate geometry: working electrode (WE) made of 0.5 cm^2 Pt plate was immersed in the electrolyte and another Pt plate of 10 cm^2 surface area was used as a counter electrode (CE). Both electrodes were produced from 99.5% purity platinum (Kultakeskus Oy, Finland), which contains impurities such as precious metals (mostly Au, Ag and Pd) and traces of base metals (Cu, Fe and Ni). A saturated calomel electrode (SCE) from SI Analytics, France, with a potential of 241 mV respective to standard hydrogen electrode was used as the reference electrode. A 24-bit potentiostat (Ivium CompactStat, Ivium Technology, Netherlands) was used to control the experiments.

2.2. Description of the EDRR process

The EDRR process is schematically shown in Figure 1. It consists of two consecutive steps, which are continuously repeated after each other. The process starts by introducing the inert working electrode into the solution (Figure 1A), which contains ions of both copper (sacrificial metal) and gold.

During the first step (Figure 1B), Cu is deposited on the electrode surface at constant cathodic potential E_{set} for a defined time t_{dep}. When the potential is applied to the electrodes, anodic reactions of oxygen and possibly also chlorine gas evolution take place:

$$\mathrm{H_2O} \longrightarrow \frac{1}{2}\mathrm{O_2} \uparrow + 2\mathrm{H^+} + 2\mathrm{e^-} \quad (1)$$

$$2\mathrm{Cl^-} \longrightarrow \mathrm{Cl_2} \uparrow + 2\mathrm{e^-} \quad (2)$$

Cathodic reaction of copper deposition on the other hand is as follows:

$$\mathrm{CuCl_4}^{3-} + \mathrm{e^-} \longrightarrow \mathrm{Cu} + 4\mathrm{Cl^-} \quad (3)$$

In the next step (Figure 1C), cell is left in open circuit conditions until the predetermined cut-off potential E_{cut} is reached. Due to the difference in their standard electrode potentials, the replacement of Cu by Au can occur:

$$\mathrm{Cu} + 4\mathrm{Cl^-} \longrightarrow \mathrm{CuCl_4}^{3-} + \mathrm{e^-} \quad (4)$$

$$\mathrm{AuCl_2}^{-} + \mathrm{e^-} \rightarrow \mathrm{Au} + 2\mathrm{Cl^-} \quad (5)$$

Overall reaction of the redox replacement step is as following:

$$\mathrm{Cu} + \mathrm{AuCl_2}^{-} + 2\mathrm{Cl^-} \longrightarrow \mathrm{Au} + \mathrm{CuCl_4}^{3-} \quad (6)$$

The redox replacement is relatively fast until the vicinity of the cathode is depleted of dissolved gold. After that, the replacement reaction is limited by the diffusion of dissolved gold towards the WE surface.

As a general rule, the higher the deposition potential E_{set} is, the more copper will deposit. This can increase the redox replacement time and/or result in higher copper content in the cathode. When the

redox reaction does not have sufficient time to fully replace existing copper, the replacement is not ideal, some traces of copper can remain in the final deposit (Figure 1D). In addition, the surface coverage might be uneven due to lattice defects or impurities on the WE surface.

In the current work, the boundaries for E_{set} and E_{cut} were determined with cyclic voltammetry (CV). The voltammograms were recorded both in the blank solution and in the gold-containing solution at scan rate v = 50 mV/s. The scan was started at 0 mV vs. SCE in anodic direction up to 1000 mV vs. SCE, then the potential was reversed until –500 mV vs. SCE was reached and the scan direction was reversed again. The second scan was used to determine characteristic peaks of the voltammograms.

2.3. Analytical techniques

The amount of gold deposited on the surface of WE was evaluated by means of cyclic voltammetry. Immediately after the end of EDRR process the electrodes were removed from working solution, rinsed with deionized water and then CV was run in a solution of 175 g/L NaCl at a scan rate v = 50 mV/s starting from the potential of 400 mV vs. SCE until 1000 mV vs. SCE. The amplitude of a gold stripping peak (in mA/cm^2) during the first sweep in anodic direction is directly related to the amount of gold deposited on the WE.

Mass of recovered Cu and Au was determined by potentiostatic dissolution of the gold deposit at 1.1 V vs. SCE in 175 g/L NaCl. Obtained solutions were analyzed with ThermoScientific iCapQ Inductively Coupled Plasma Mass-Spectrometer (ICP-MS).

The replacement of Cu by Au and the surface coverage were investigated by X-ray photoelectron spectroscopy (XPS). XPS measurements were carried out with a KRATOS Axis Ultra (Kratos Analytical, Manchester, United Kingdom) with a monochromatic Al X-ray source operating at 100 W. The analysis spot size is 400 × 800 µm. The samples were analyzed under ultra-high vacuum in pressure range of 10^{-8} – 10^{-9} Torr at room temperature. Each analysis started with a survey scan from 0 to 1100 eV binding energy using a pass energy of 80 eV at steps of 1 eV that led to the emission of photoelectrons from the top 10-20 nm of the surface. High-resolution spectra of Cu2p and Au4f (and Pt 4f due to using Pt as a substrate material) were collected at 20 eV pass energy at steps of 0.1 eV and 300 ms dwell time with 8 and 4 sweeps, respectively. Binding energies were charge-corrected by referencing to adventitious carbon at 285.0 eV and a piece of fresh pure cellulose paper was used as the in-situ reference. CasaXPS software was used for peak fitting and analysis.

Morphology of deposit was studied using Scanning Electron Microscope (SEM) Carl Zeiss LEO 1450 VP, Germany, equipped with an Energy Dispersion X-ray spectroscopy (EDS) INCA software from Oxford Instruments, UK. The applied acceleration voltage and the beam intensity were 15 kV and 210-240 pA,

respectively. Prior to SEM-EDS analysis, the samples were rinsed with deionized water and air-dried at room temperature.

2.4. Experimental design

Two solutions with elevated gold and chloride concentrations (Solutions 1 and 2, Table 1) were used for studying the influence of process variables on the gold deposition process. Estimation of the gold amount deposited on the electrode surface in different tests was done in semi-quantitative way by comparing the current density j_{max} of gold oxidation peak on a voltammogram recorded straight after the EDRR. In order to determine the impact of the parameters on the gold recovery in the process, a full factorial test was designed and analyzed with the MODDE 12.0 software. The investigated factors include concentration of gold *[Au]* in the solution, time t_{dep} and potential E_{set} for copper deposition and cut-off potential E_{cut}. In total 16 combinations of parameters were studied (E1-E16 in Table 2). The order in which the experiments were made was randomized to avoid systematic errors. The experimental results were assessed statistically by the coefficient of determination (R^2), standard errors of model coefficient (Student's *t*-test) and the analysis of variance (ANOVA) using Fisher's variance ratio test (*F*-test).

Solution 3 (Table 1) has the composition close to one obtained from chloride containing leaching process of WEEE (Elomaa et al., 2017) and it was used in the search of the optimal set of parameters with a response surface methodology (RSM). For that purpose, a central composite face-centered design of experiments was built with three factors: t_{dep}, E_{set} and E_{cut} (Table 3). Such experimental plan requires less tests than full factorial design and enables introduction of quadratic terms into the regression model to describe the curvature of response surface, providing at the same time acceptable quality of predictions (Eriksson et al., 2008). The purpose of the central composite design is to fit the second-order model correlating the EDRR parameters and the composition of deposit. The central point was replicated twice in order to provide a most adequate prediction in all the experimental region and evaluate the pure error between each repetition.

The optimized process parameters were then used for producing thicker deposits on the WE by extending the number of EDRR cycles up to 250. In order to improve diffusion between electrodes, stirring of about 100 rpm was applied to the solution with a magnetic stirrer.

2.5. Efficiency indicators

Efficiency of the EDRR process was assessed by the current efficiency and specific energy consumption. Current efficiency η, %, achieved in the experiments was calculated according to Moats (2018):

$$\eta = \frac{I_{theor}}{I_{real}} \cdot 100\%, \quad (7)$$

where I_{real} – current measured in the experiment, A;

I_{theor} – theoretical current determined from Faraday's law:

$$I_{theor} = \frac{z \cdot F \cdot m}{M \cdot t_{dep} \cdot N} \quad (8)$$

where z – number of electrons involved in the reaction;

F = 96485 A·s/mol – Faraday constant;

m – mass of the recovered metal, g;

M – molar mass of the metal, g/mol;

N – number of EDRR cycles.

Since the potential was applied to the cell only during the deposition step, specific energy consumption w, kWh/kg Au, can be calculated as follows (Moats, 2018):

$$w = \frac{E_{cell} \cdot I_{real} \cdot t_{dep} \cdot N}{3600 \cdot m_{Au}} \quad (9)$$

where E_{cell} – cell voltage measured between working and counter electrodes, V;

m_{Au} – mass of the recovered gold, g.

3. Results and discussion

3.1. Background experiments

In order to determine the range of operating parameters, cyclic voltammetry experiments with the blank solution (175 g/L NaCl and 1.2 g/L Cu, Table 1) and the same solution containing 100 mg/L of gold (Solution 1, Table 1) were carried out, Figure 2. The mechanism of reactions occurring in similar system during the potential sweep was detailed by Lekka *et al.* (2015).

In both solutions (Figure 2) the anodic peak (***a₂***) at 320 mV vs. SCE and the corresponding cathodic peak (***c₂***) at 250 mV vs. SCE were observed, which refer to a reversible cupric-cuprous redox reaction at the electrode surface involving only dissolved species. According to Muir (2002), in solutions with high salinity ($[Cl^-] > 1$ M) the prevailing cuprous and cupric species are $CuCl_4^{3-}$ and $CuCl^+$ respectively. Thus, the suggested overall reaction is:

$$CuCl_4^{3-} \rightleftharpoons CuCl^+ + 3Cl^- + e^- \quad (10)$$

The cathodic peak (***c₁***) at –300 mV vs. SCE and the respective anodic peak (***a₁***) at –140 mV vs. SCE have distinct deposition/stripping shape. Rapid current increase during scan in cathodic direction indicates the deposition of elemental copper on the electrode surface:

$$\mathrm{CuCl_4}^{3-} + \mathrm{e}^- \longrightarrow \mathrm{Cu} + 4\mathrm{Cl}^- \quad (11)$$

After reaching the cathodic peak ***c₁***, the current decayed due to the depletion of copper ion species in proximity of the electrode surface. Once the scan direction was reversed at –500 mV vs. SCE, the current began to rise gradually because of copper stripping followed by its complexation with chloride ions. Sharp current drop after the anodic peak ***a₁*** at –140 mV vs. SCE denotes dissolution of copper layer from the surface of cathode:

$$\mathrm{Cu} + \mathrm{Cl}^- \longrightarrow \mathrm{CuCl_{(ads)}} + \mathrm{e}^- \quad (12)$$

$$\mathrm{CuCl_{(ads)}} + 3\mathrm{Cl}^- \longrightarrow \mathrm{CuCl_4}^{3-} \quad (13)$$

Unlike in the case of blank solution, the voltammogram for the gold-containing Solution 1 exhibits a minor oxidation peak at 750 mV vs. SCE (***a₃***). Since the only difference between two studied solutions is in presence of gold, this peak was assigned to reaction of gold stripping from the electrode surface. Heumann and Panesar (1965) showed that both Au(I) and Au(III) species are produced by oxidation of gold in presence of chloride. Recent studies (Lampinen et al., 2017; Seisko et al., 2017) on the mechanism of gold dissolution in chloride media demonstrated that under the conditions of this study ($[Cl^-]$ = 175 g/L, $[Cu^{2+}]$ = 1.2 g/L, T = 25°C) gold dissolves predominantly in the form of $AuCl_2^-$ complex:

$$\mathrm{Au} + 2\mathrm{Cl}^- \rightleftharpoons \mathrm{AuCl_2}^- + \mathrm{e}^- \quad (14)$$

However, the corresponding cathodic peak ***c₃*** was not detected at applied scan rate due to fairly slow kinetics of gold deposition caused by formation of gold chlorocomplex and low concentration of $AuCl_2^-$ ions in the solution.

Based on these observations, the aimed deposition of sacrificial copper layer was identified at potential in the range between –250 mV and –500 mV vs. SCE (Figure 2). At more cathodic potential, hydrogen evolution will decrease the efficiency of the metal deposition reaction, as a portion of the used charge will be spent for hydrogen gas formation. Moreover, the formation of H_2 gas will reduce the adhesion of deposited metal on the surface, leading to non-uniform morphology. The cut-off potential (i.e. the open circuit potential which the electrode must reach before the next cycle can commence) must allow sufficient time for the redox replacement reaction to proceed, but shall not exceed 600 mV vs. SCE to prevent gold stripping from the cathode. The designated cut-off potential for redox replacement reactions has a strong effect on the composition of the coating as interrupting

the reaction before all metal ions in sacrificial layer has been replaced leads to an alloy of the two metals (Jayaraju et al., 2014; Mercer et al., 2015).

For the studied electrochemical system, the operating range for E_{set} was between –500 and –250 mV vs. SCE and E_{cut} range was between 0 and 600 mV vs. SCE.

3.2. Electrodeposition followed by redox replacement

Figure 3 shows the typical profile of the potential as a function of time during the EDRR process. The curve shows both the deposition step at E_{set} = –500 mV vs. SCE for 10 s followed by open-cell potential until the cut-off potential E_{cut} = 0 mV vs. SCE was reached and the next cycle could commence. The entire process consisting of 10 cycles of EDRR takes less than 400 s. After the end of last cycle, the voltammogram was recorded in the 175 g/L NaCl solution at 50 mV/s to confirm the formation of gold layers on the cathode surface (Figure 4). For the purpose of clarity, the results of EDRR experiments aimed to study of the impact of process parameters are described on the example of one typical test, E11 (Table 2). The results for complete set of experiments are provided in the Supplementary Material (Figures S1-S16).

The large spike in the beginning of the voltammogram after electrodeposition (ED) only is attributed to the instantaneous dissolution of major amount of copper deposited on WE at the anodic potential of 400 mV vs. SCE. The presence of the current peak $\boldsymbol{a_3}$ between 750 and 800 mV vs. SCE, on the other hand, corresponds to the oxidation of gold (aka stripping of gold) as described in Section 3.1; therefore it can be concluded that also small amount of Au is co-deposited in ED step. In contrast, the current density after EDRR in the beginning of CV profile is much lower than after pure ED suggesting that less copper is present in the deposit: this is an expected result as during the redox replacement step Cu is dissolved back to solution and Au is enriched to the electrode.

The current density of gold oxidation peak $\boldsymbol{a_3}$ was shown to be remarkable higher after EDRR than either in the background experiments or after pure ED. This confirms that EDRR was successful and gold was enriched on the cathode in the process. It is worth noting that dissolution of deposit increased local concentration of gold ions near the electrode surface that resulted in its reduction during the reverse scan of CV. It is reflected on the voltammogram by a minor cathodic peak $\boldsymbol{c_3}$ around 550 mV vs. SCE.

Extent of Cu and Au co-deposition was investigated by performing only ED, without a redox replacement step, i.e. applying potential E_{set} = –300 mV vs. SCE for 100 s; this is comparable to a typical electrowinning procedure. Comparison of the results with the composition of the deposit obtained after EDRR (Table 4) clearly indicate the co-deposition of copper and gold during ED step. Moreover, Table 4 also shows that the redox replacement step substantially increases the amount of recovered

gold on the expense of copper, thus improving the Au content in the product up to 5 times. This result truly shows the power of EDRR process when compared to pure electrowinning, especially as RR step is performed in the absence of applied potential or current, i.e. this 5-fold increase in the Au recovery is obtained without additional energy consumption. The similar behavior was discovered in all the EDRR tests, showing also how EDRR can be easily adjusted to the solution composition by simply adjusting the EDRR parameters.

3.3. Optimization of EDRR process parameters for gold recovery

The influence of parameters t_{dep}, E_{set}, E_{cut}, *[Au]* and any two-way interactions between them on j_{max} (i.e. the gold oxidation peak in stripping CV) was investigated using multiple linear regression model.

Table 5 displays coefficients of the model and their effect on Au recovery (determined from Au stripping peak), standard deviation of each coefficient and *p*-values for the full factorial design. The positive coefficients reveal that the increase of corresponding parameters increased j_{max}, and conversely, negative values decreased the response. In addition, the model yielded a coefficient of determination R^2_{adj} of 0.966 and model validity of 0.73, which indicates that conclusions drawn based on this model were statistically sound.

As it can be seen, besides the apparent effect of the gold concentration (8–100 mg/L) on the peak current, the cut-off potential (0–600 mV vs. SCE) and its combination with gold concentration was shown to have a substantial impact on gold layer formation while the copper deposition time t_{dep} (1–20 s) influences the peak intensity to the lesser extent. In general, shorter deposition time produces smaller amount of copper available on the cathode surface for gold redox replacement. The same motivation applies for low deposition potentials at which the rate of copper reduction is fairly slow. However, E_{set} and all derived terms had no effect at the 95% confidence level ($p > 0.05$). This is most likely because the concentration of gold is a limiting factor in the given conditions, meaning that the amount of the reduced copper available for the redox replacement is excessive with regard to the gold ions in solution.

In order to ensure the appropriate model, the variance analysis (ANOVA) was performed. According to Table 6, the *F*-ratio of the mean sum of squares (MS) was found to be smaller than the table value of 6.61 that implies no lack of fit. The significance of the regression model was tested using the ratio of the mean sum of squares for regression and residual. The calculated ratio was found to be greater than the critical *F*-value (4.06) indicating that the regression is significant at a confidence level of 95%.

The peak current densities j_{max} obtained from the process optimization tests with central composite face-centered experimental design are represented in relation to t_{dep}, E_{set}, E_{cut}, in Table 3. The highest anodic current density of 60.1 mA/cm^2 was achieved after copper deposition for 5 s at –375 mV vs.

SCE followed by the redox replacement by gold until the open circuit potential reached 600 mV vs. SCE. A difference of nearly 1 V between copper deposition potential and cut-off potential provides enough time for gold ions to effectively replace copper at the surface. At the lower cut-off potentials, less gold was deposited on WE due to the shorter period of the redox replacement, which results in smaller gold oxidation peak on the voltammogram.

The resulting response surface model is expressed by the following equation:

$$\log j_{max} = -0.214 + 0.245 \cdot t_{dep} + 2.17 \cdot 10^{-4} \cdot E_{cut} - 0.012 \cdot t_{dep}^2 + 2.98 \cdot 10^{-6} \cdot E_{cut}^2 - 1.03 \cdot \\ \cdot 10^{-4} \cdot t_{dep} \cdot E_{cut}$$

Notably, since the E_{set} did not have statistically valid effect on the gold oxidation current, it was eliminated from the model. Afterwards, the fitted model was checked with ANOVA for adequacy of fit (Table 7) in the region defined by the design matrix and was found to be reliable at 95% confidence level. A 3D response surface plot of the predicted model is presented in Figure 5. It suggests that regardless of the high goodness of fit, there is still some deviation of the regression model from the experimental data points, especially close to the maximum current density. Due to this reason, two points for confirmation experiments L1 and L2 (Table 8) with extended number of EDRR cycles were selected around the predicted maximum of response surface, with E_{cut}, = 550 mV vs. SCE and t_{dep} = 5 and 10 s, respectively. The deposition potential E_{set} was set to -325 mV vs. SCE which is slightly lower than the copper deposition peak $\boldsymbol{c_1}$ (Figure 2).

3.4. Gold recovery and energy consumption

The recovery of gold and copper in validation tests L1 and L2 (Table 8) was quantified by dissolving the WE samples in concentrated aqua regia ($HCl:HNO_3$ = 3:1) and assaying the produced solution for Au and Cu with ICP-MS (Table 8). As the material of working electrodes also contains traces of gold and copper, the chemical assays were corrected for the background concentrations, which were obtained by applying the same analytical procedure to a sample of uncovered electrode material. In both tests selective recovery of gold was observed. The ratio between Au and Cu increased from 1:340 in the initial solution (Table 1) up to 1.1:1 in test L2 and 3.3:1 in test L1 (Table 8). However, higher purity of the gold deposit corresponds to its lower recovery from the solution.

The current efficiency observed in these tests varied around 40%. Since the potential was only applied during the ED step, the current efficiency refers to that of Cu and partial co-deposition of Au during this step. In addition, the energy consumption was calculated, and the obtained values are 114.3 kWh/kg Au at recovery of 8.4% and 292.9 kWh/kg Au at recovery of 9.3% in test L1 and L2, respectively. It is also worth noting that the optimization in this study was not performed with respect

to the energy consumption but instead, to the enrichment of Au on the electrode surface. Thus, utilizing more positive E_{set} could in reality result in much lower specific energy consumption.

When comparing these values to the electrowinning, EDRR shows a comparable performance, especially in the case of the current efficiency. For example, the study by Brandon *et al*. (1987) reported 112 kWh/kg energy consumption and only 0.33% current efficiency in 5 ppm Au (cyanide) solution. Kasper *et al*. (2018), on the other hand, have studied gold electrowinning from thiosulfate solutions and achieved a current efficiency of 1-6% for 100 ppm Au solution and values less than 1% for 10 ppm Au solution. Therefore, the clearly higher current efficiency (40% for 8 ppm Au solution) of EDRR is attributed to the redox replacement step, during which no external potential or current is applied, even if the majority of the recovery takes place during this step. In contrast to the current efficiency, Kasper *et al*. (2018) achieved the gold recovery with low energy consumption (5-15 kWh/kg, depending on the applied potential, after approx. 300 min process) from 100 ppm Au solution. However, it is important to point out that the solution studied by Kasper *et al.* (2018) contained over a decade higher gold concentration (100 ppm) when compared to the EDRR study (8 ppm), and lower the Au concentration, higher the energy consumption is: a direct comparison between these values is difficult as Kasper *et al*. (2018) do not report energy consumption for the 10 ppm Au solutions. Nevertheless, these results indicate that at higher gold concentrations, the optimized EW might result in lower energy consumption while EDRR is a competitive option for solutions containing only trace amounts of Au. Also, a full optimization of the EDRR system can further improve the energy consumption.

3.5. Surface characterization

In order to quantify the surface coverage, XPS measurements were performed. The presence of surface contaminants, carbon and oxygen, formed by air exposure and hydrocarbon contamination is common for all sample surfaces. However, some of the oxygen can be attributed to the formation of metal oxide products. The high resolution spectra of Au4f and Cu2p regions from the deposit and Pt4f regions from the substrate material are demonstrated in Figure 6.

As expected, clean substrate material (Figure 6A) showed strong peaks for Pt at 71.14 eV (Pt $4f_{7/2}$) and 74.45 eV (Pt $4f_{5/2}$) but only marginal signal of Au and Cu impurities were observed. In contrast, on the test samples clear Au peaks at 83.88 eV (Au $4f_{7/2}$) and 87.56 eV (Au $4f_{5/2}$) were detected. These peak positions and distances between spin-orbit components are corroborated by those found in literature for Pt and Au (NIST, 2012). No quantifiable amount of Cu was detected on the surface up to 20 nm depth. This indicates complete redox replacement of copper with gold at least in the outermost

surface layers. As the process consists of identical cycles, it is expected that all the deposit formed has same composition as the surface layers.

SEM micrographs of the WE surface (Figure 7) after EDRR revealed a uniform layer of material composed mostly of gold and unevenly distributed gold clusters all over the immersed part of the electrode. The cross section of the WE exhibits loosely attached porous buildup with micro-cavities which are a result of dissolution of initially deposited copper. It is worth noting that such texture is typical for deposits obtained from liquid phase and it is comparable to the product of conventional gold electrowinning (Steyn and Sandenbergh, 2004).

3.6. Advantages and disadvantages of EDRR

Electrolysis for base metals in chloride media is a state-of-art process in metallurgy and in industrial practice the potentially hazardous side reaction of chlorine gas formation has been turned into advantage. For example, at Glencore Nikkelverk refinery Cl_2 produced in Ni and Co tankhouse is collected and introduced back into leaching tanks, where it reacts with the feed material dissolving base metals and heating up the slurry due to the exothermic nature of the reaction (Stensholt et al., 2001). In the HydroCopper process developed by Outokumpu (Hyvärinen et al., 2004), on the other hand, the generated chlorine gas by chlor-alkali electrolysis is used in copper chloride leaching.

Similarly to other electrochemical processes performed in chloride media, the proposed EDRR method may also produce Cl_2 in an anodic side-reaction and if not treated and collected properly, it can be hazardous and toxic. However, similar to abovementioned commercial processes, Cl_2 offers a potential advantage in the Au chloride leaching process. This fact is even further enhanced as EDRR can be applied directly after leaching, thus leaving out an activated carbon and all unit operations related to its treatment – adsorption, elution and regeneration.

Moreover, EDRR process parameters (E_{set}, E_{cut}, t_{dep}, number of cycles) can be controlled and changed relatively easily – without additional chemical – to reflect the raw material variations and subsequent Au:Cu ratios present in the solution after leaching step. Therefore, the presented method can contribute in elimination or reduction of toxic and hazardous substances typically used in mining operations. Also, the product morphology compares to one obtained by conventional electrowinning (Steyn and Sandenbergh, 2004), hence the following steps such as mechanical cathode stripping, chemical or electrochemical dissolution, smelting and refining Doré bars (Marsden and House, 2006; Stange, 1999) in production chain will be the same for both technologies.

Overall, utilizing EDRR could reduce the need for resources and the costs related to entire gold recovery process. However, the detailed investigation of energy efficiency and energy consumption of this particular process is the subject of future studies, while this paper clearly proves the feasibility

of EDRR process for the Au:Cu process in chloride media. Moreover, due to the spontaneous nature of redox replacement there is a clear indication that the EDRR is more effective than for example electrowinning when the noble metal is present in solution at very low concentration (Halli et al., 2017).

4. Conclusions

This study demonstrates the feasibility and optimization of electrodeposition-redox replacement (EDRR) method for the recovery of gold from chloride solutions containing only very dilute amounts of gold. First, copper is electrodeposited at constant potential during brief period of time (1-10 s), after which the potential is switched to the open-circuit condition for redox replacement reaction to proceed until a pre-determined cut-off potential is achieved. It was found that the difference between these two potential values and concentration of both metals have strong impact on the end result.

It was shown that when the cell is left at the open circuit condition after the copper deposition step, two simultaneous processes occur at the surface of WE: 1) copper starts to dissolve from electrode followed by increase in the electrode potential, and 2) gold is deposited on the WE, due to charge transfer i.e. "cementation reaction" between reduced copper and dissolved gold species. EDRR proved effective in the recovery of Au when EDRR method was compared to electrowinning (i.e. pure electrodeposition and no redox replacement), as EDRR process yields a product with content of Au of 37.2% in comparison to 7.8% in conventional electrowinning. The composition of the deposited alloy can be tuned by adjusting potential values of E_{set} and E_{cut}.

Also, 1000-fold enhancement was observed in Au:Cu ratio (1:340 in solution *cf.* 3.3:1 on the cathode surface) when 250 EDRR cycles were performed at optimized conditions: t_{dep} = 5 s, E_{set} = –325 mV vs. SCE and E_{cut}, = 550 mV vs. SCE. This translates to 8.4% Au recovery from the solution and when taking into account that the starting concentration is 8 mg/L of Au and 2.7 g/L Cu, this is truly a testament of EDRR's effectiveness.

All in all, the obtained results prove that the EDRR method can be productively used for the recovery of trace amounts of gold from cupric chloride solutions used for cyanide-free gold leaching in environmentally friendly and resource-efficient manner.

Acknowledgements

This research has received funding from the European Union Framework Program for Research and Innovation Horizon 2020 under Grant Agreement No. 721385 (EU MSCA-ETN SOCRATES; project

website: http://etn-socrates.eu) and NoWASTE project (No. 297962) by Academy of Finland. In addition, Emil Aaltonen Foundation, "RawMatTERS Finland Infrastructure" (RAMI) by Academy of Finland and METSEK project funded by Association of Finnish Steel and Metal Producers are greatly acknowledged. The authors appreciate involvement of Dr. Mari Lindgren (Outotec Research Center, Pori) with experiments set-up and thank Dr. Leena-Sisko Johansson from Aalto University Department of Bioprocesses and Biosystems for performing the XPS analysis.

References

Adams, M.D., 2016. Chloride as an Alternative Lixiviant to Cyanide for Gold Ores, in: Adams, M.D. (Ed.), Gold Ore Processing. Elsevier B.V., Amsterdam, The Netherlands, pp. 525–531. doi:10.1016/B978-0-444-63658-4.00029-3

Ahtiainen, R., Lundström, M., 2016. Preg-robbing of Gold in Chloride-Bromide Solution. Physicochemical Problems of Mineral Processing 52, 244–251. doi:10.5277/ppmp160121

Al Amri, Z., Mercer, M.P., Vasiljevic, N., 2016. Surface Limited Redox Replacement Deposition of Platinum Ultrathin Films on Gold: Thickness and Structure Dependent Activity towards the Carbon Monoxide and Formic Acid Oxidation reactions. Electrochimica Acta 210, 520–529. doi:10.1016/j.electacta.2016.05.161

Baghalha, M., 2007. Leaching of an oxide gold ore with chloride/hypochlorite solutions. International Journal of Mineral Processing 82, 178–186. doi:10.1016/j.minpro.2006.09.001

Benson, D.M., Tsang, C.F., Sugar, J.D., Jagannathan, K., Robinson, D.B., El Gabaly, F., Cappillino, P.J., Stickney, J.L., 2017. Enhanced Kinetics of Electrochemical Hydrogen Uptake and Release by Palladium Powders Modified by Electrochemical Atomic Layer Deposition. ACS Applied Materials & Interfaces 9, 18338–18345. doi:10.1021/acsami.7b03005

Binnemans, K., Jones, P.T., 2017. Solvometallurgy: An Emerging Branch of Extractive Metallurgy. Journal of Sustainable Metallurgy 3, 570–600. doi:10.1007/s40831-017-0128-2

Bisceglie, F., Civati, D., Bonati, B., Faraci, F.D., 2017. Reduction of potassium cyanide usage in a consolidated industrial process for gold recovery from wastes and scraps. Journal of Cleaner Production 142, 1810–1818. doi:10.1016/j.jclepro.2016.11.103

Brandon, N.P., Mahmood, M.N., Page, P.W., Roberts, C.A., 1987. The direct electrowinning of gold from dilute cyanide leach liquors. Hydrometallurgy 18, 305–319. doi:10.1016/0304-386X(87)90072-7

Brankovic, S.R., Wang, J.X., Adžić, R.R., 2001a. Pt Submonolayers on Ru Nanoparticles: A Novel Low Pt Loading, High CO Tolerance Fuel Cell Electrocatalyst. Electrochemical and Solid-State Letters 4, A217–A220. doi:10.1149/1.1414943

Brankovic, S.R., Wang, J.X., Adžić, R.R., 2001b. Metal monolayer deposition by replacement of metal adlayers on electrode surfaces. Surface Science 474, L173–L179. doi:10.1016/S0039-6028(00)01103-1

Calvo, G., Mudd, G.M., Valero, A., Valero, A., 2016. Decreasing Ore Grades in Global Metallic Mining: A Theoretical Issue or a Global Reality? Resources 5, 36. doi:10.3390/resources5040036

Deschênes, G., 2016. Advances in the Cyanidation of Gold, in: Adams, M.D. (Ed.), Gold Ore Processing. Elsevier B.V., Amsterdam, The Netherlands, pp. 429–445. doi:10.1016/B978-0-444-63658-4.00026-8

Dimitrov, N., 2016. Recent Advances in the Growth of Metals, Alloys, and Multilayers by Surface Limited Redox Replacement (SLRR) Based Approaches. Electrochimica Acta 209, 599–622. doi:10.1016/j.electacta.2016.05.115

Elomaa, H., Seisko, S., Junnila, T., Sirviö, T., Wilson, B.P., Aromaa, J., Lundström, M., 2017. The Effect of the Redox Potential of Aqua Regia and Temperature on the Au, Cu, and Fe Dissolution from WPCBs. Recycling 2, 14. doi:10.3390/recycling2030014

Eriksson, L., Johansson, E., Kettaneh-Wold, N., Wikström, C., Wold, S., 2008. Design of experiments: principles and applications, 3rd ed. Umetrics Academy, Umeå, Sweden.

Fayette, M., Liu, Y., Bertrand, D., Nutariya, J., Vasiljevic, N., Dimitrov, N., 2011. From Au to Pt via Surface Limited Redox Replacement of Pb UPD in One-Cell Configuration. Langmuir 27, 5650–5658. doi:10.1021/la200348s

Ferron, C.J., Fleming, C.A., Dreisinger, D.B., O'Kane, T., 2003. Chloride As an Alternative To Cyanide for the Extraction of Gold - Going Full Circle?, in: Young, C.A., Alfantazi, A.M., Anderson, C.G., Dreisinger, D.B., Harris, B., James, A. (Eds.), Hydrometallurgy 2003: 5th International Conference in Honor of Prof. I.M. Ritchie. The Minerals, Metals & Materials Society, Vancouver, BC, Canada, pp. 89–104.

Forsén, O., Aromaa, J., 2013. The use of hydrometallurgy in treatment of secondary raw materials and low-grade ores. Acta Metallurgica Slovaca 19, 184–195. doi:10.12776/ams.v19i3.160

Habashi, F., 2016. Gold – An Historical Introduction, in: Adams, M.D. (Ed.), Gold Ore Processing. Elsevier B.V., Amsterdam, The Netherlands, pp. 1–20. doi:10.1016/B978-0-444-63658-4.00001-3

Halli, P., Elomaa, H., Wilson, B.P., Yliniemi, K., Lundström, M., 2017. Improved Metal Circular Economy – Selective Recovery of Minor Ag Concentrations from Zn Process Solutions. ACS Sustainable Chemistry & Engineering 5, 10996–11004. doi:10.1021/acssuschemeng.7b02904

Hasab, M.G., Rashchi, F., Raygan, S., 2014. Chloride–hypochlorite leaching and hydrochloric acid washing in multi-stages for extraction of gold from a refractory concentrate. Hydrometallurgy 142, 56–59. doi:10.1016/j.hydromet.2013.11.015

Heumann, T., Panesar, H.S., 1965. Beitrag zur Frage nach dem Auflösungsmechanismus von Gold zu Chlorkomplexen und nach seiner Passivierung. Zeitschrift für Physikalische Chemie 229, 84–97. doi:10.1515/zpch-1965-22910

Hormozi Nezhad, M.R., Aizawa, M., Porter, L.A., Ribbe, A.E., Buriak, J.M., 2005. Synthesis and patterning of gold nanostructures on InP and GaAs via galvanic displacement. Small 1, 1076–1081. doi:10.1002/smll.200500121

Hyvärinen, O., Hämäläinen, M., Lamberg, P., Liipo, J., 2004. Recovering gold from copper concentrate via the HydroCopper^{TM} process. JOM 56, 57–59. doi:10.1007/s11837-004-0184-5

Jayaraju, N., Banga, D., Thambidurai, C., Liang, X., Kim, Y.-G., Stickney, J.L., 2014. PtRu Nanofilm Formation by Electrochemical Atomic Layer Deposition (E-ALD). Langmuir 30, 3254–3263. doi:10.1021/la403018v

Jenkin, G.R.T., Al-Bassam, A.Z.M., Harris, R.C., Abbott, A.P., Smith, D.J., Holwell, D.A., Chapman, R.J., Stanley, C.J., 2016. The application of deep eutectic solvent ionic liquids for environmentally-friendly dissolution and recovery of precious metals. Minerals Engineering 87, 18–24. doi:10.1016/j.mineng.2015.09.026

Jin, Y., Shen, Y., Dong, S., 2004. Electrochemical Design of Ultrathin Platinum-Coated Gold Nanoparticle Monolayer Films as a Novel Nanostructured Electrocatalyst for Oxygen Reduction. The Journal of Physical Chemistry B 108, 8142–8147. doi:10.1021/jp0375517

Kasper, A.C., Veit, H.M., García-Gabaldón, M., Herranz, V.P., 2018. Electrochemical study of gold recovery from ammoniacal thiosulfate, simulating the PCBs leaching of mobile phones. Electrochimica Acta 259, 500–509. doi:10.1016/j.electacta.2017.10.161

Kirke Rose, T., 1894. The Metallurgy of Gold. C. Griffin Ltd., London, United Kingdom.

Lampinen, M., Seisko, S., Forsström, O., Laari, A., Aromaa, J., Lundström, M., Koiranen, T., 2017. Mechanism and kinetics of gold leaching by cupric chloride. Hydrometallurgy 169, 103–111. doi:10.1016/j.hydromet.2016.12.008

Leikola, M., Elomaa, H., Jafari, S., Rintala, L., Wilson, B.P., Lundström, M., 2017. Cyanide-free future of gold process selection, in: Taylor, A. (Ed.), ALTA 2017 Gold & Precious Metals Conference. Perth, WA, Australia, pp. 232–241.

Lekka, M., Masavetas, I., Benedetti, A.V., Moutsatsou, A., Fedrizzi, L., 2015. Gold recovery from waste electrical and electronic equipment by electrodeposition: A feasibility study. Hydrometallurgy 157, 97–106. doi:10.1016/j.hydromet.2015.07.017

Lemieux, D., Lalancette, J.-M., Dubreuil, B., 2013. Treatment of a Gold Refractory Concentrate with Halogens, in: 23rd World Mining Congress. Canadian Institute of Mining, Metallurgy and Petroleum, Montréal, QC, Canada, p. 364.

Leppinen, J.O., Hämäläinen, M., Hyvärinen, O., 2005. Chloride leaching of gold from sulfide concentrates, in: Deschênes, G., Hodouin, D., Lorenzen, L. (Eds.), 1st International Symposium on Treatment of Gold Ores. Canadian Institute of Mining, Metallurgy and Petroleum, Calgary, AB, Canada, pp. 165–175.

Lu, Y., Song, Q., Xu, Z., 2017. Integrated technology for recovering Au from waste memory module by chlorination process: Selective leaching, extraction, and distillation. Journal of Cleaner Production 161, 30–39. doi:10.1016/j.jclepro.2017.05.033

Lundström, M., Ahtiainen, R., Haakana, T., O'Callaghan, J., 2014. Techno-economical observations related to Outotec Gold Chloride process, in: Taylor, A. (Ed.), ALTA 2014 Gold & Precious Metals Conference. Perth, WA, Australia, pp. 89–104.

Lundström, M., Liipo, J., Aromaa, J., 2012. Dissolution of copper and iron from sulfide concentrates in cupric chloride solution. International Journal of Mineral Processing 102–103, 13–18. doi:10.1016/j.minpro.2011.11.005

Machado, S.A.S., Tanaka, A.A., Gonzalez, E.R., 1991. Underpotential deposition of copper and its influence in the oxygen reduction on platinum. Electrochimica Acta 36, 1325–1331. doi:10.1016/0013-4686(91)80012-W

Marsden, J.O., House, C.I., 2006. Chemistry of Gold Extraction, 2nd ed. Society for Mining, Metallurgy & Exploration, Littleton, CO, United States.

Mercer, M.P., Plana, D., Fermín, D.J., Morgan, D., Vasiljevic, N., 2015. Growth of Epitaxial Pt-Pb Alloys by Surface Limited Redox Replacement and Study of Their Adsorption Properties. Langmuir 31, 10904–10912. doi:10.1021/acs.langmuir.5b02351

Miettinen, V., Haapalainen, M., Ahtiainen, R., Karonen, J., 2013. Development of gold chloride process, in: Taylor, A. (Ed.), ALTA 2013 Gold Conference. Perth, WA, Australia, pp. 187–202.

Mitchell, C., Fayette, M., Dimitrov, N., 2012. Homo- and hetero-epitaxial deposition of Au by surface limited redox replacement of Pb underpotentially deposited layer in one-cell configuration. Electrochimica Acta 85, 450–458. doi:10.1016/j.electacta.2012.08.024

Moats, M.S., 2018. Energy Efficiency of Electrowinning, in: Awuah-Offei, K. (Ed.), Energy Efficiency in the Minerals Industry, Green Energy and Technology. Springer International Publishing, Cham, Switzerland, pp. 213–232. doi:10.1007/978-3-319-54199-0_12

Moyes, J., Houllis, F., Huens, J.-L., Sammut, D., 2005. The Intec Gold Process - A halide-based alternative for the recovery of gold from refractory sulphide deposits, in: Deschênes, G., Hodouin, D., Lorenzen, L. (Eds.), 1st International Symposium on Treatment of Gold Ores. Canadian Institute of Mining, Metallurgy and Petroleum, Calgary, AB, Canada, pp. 177–192.

Mudd, G.M., 2007. Global trends in gold mining: Towards quantifying environmental and resource sustainability. Resources Policy 32, 42–56. doi:10.1016/j.resourpol.2007.05.002

Muir, D.M., 2002. Basic principles of chloride hydrometallurgy, in: Peek, E.M.L., van Weert, G. (Eds.), Chloride Metallurgy 2002: Practice and Theory of Chloride/Metal Interaction. Canadian Institute of Mining, Metallurgy and Petroleum, Montréal, QC, Canada, pp. 759–791.

Nam, K.S., Jung, B.H., An, J.W., Ha, T.J., Tran, T., Kim, M.J., 2008. Use of chloride–hypochlorite leachants to recover gold from tailing. International Journal of Mineral Processing 86, 131–140. doi:10.1016/j.minpro.2007.12.003

NIST, 2012. X-ray Photoelectron Spectroscopy Database, Version 4.1 [WWW Document]. URL http://srdata.nist.gov/xps (accessed 6.30.17).

Pangum, L.S., Browner, R.E., 1996. Pressure chloride leaching of a refractory gold ore. Minerals Engineering 9, 547–556. doi:10.1016/0892-6875(96)00042-8

Park, S.-M., Shin, S.-Y., Yang, J.-S., Ji, S.-W., Baek, K., 2015. Selective Recovery of Dissolved Metals from Mine Drainage Using Electrochemical Reactions. Electrochimica Acta 181, 248–254. doi:10.1016/j.electacta.2015.03.085

Seisko, S., Forsström, O., Aromaa, J., Lundström, M., 2017. Dissolution of Gold in Ferric and Cupric Chloride Solutions, in: Waschki, U. (Ed.), European Metallurgical Conference (EMC 2017). GDMB Verlag GmbH, Leipzig, Germany, pp. 19–30.

Sheridan, L.B., Gebregziabiher, D.K., Stickney, J.L., Robinson, D.B., 2013. Formation of Palladium Nanofilms Using Electrochemical Atomic Layer Deposition (E-ALD) with Chloride Complexation. Langmuir 29, 1592–1600. doi:10.1021/la303816z

Stange, W., 1999. The process design of gold leaching and carbon-in-pulp circuits. Journal of the South African Instute of Mining and Metallurgy 99, 13–26.

Stensholt, E.O., Dotterud, O.M., Henriksen, E.E., Ramsdal, P.O., Stålesen, F., Thune, E., 2001. Development and practice of the Falconbridge chlorine leach process. CIM Bulletin 94, 101–104.

Steyn, J., Sandenbergh, R.F., 2004. A study of the influence of copper on the gold electrowinning process. Journal of The South African Institute of Mining and Metallurgy 104, 177–182.

Sun, Y., Xia, Y., 2004. Mechanistic Study on the Replacement Reaction between Silver Nanostructures and Chloroauric Acid in Aqueous Medium. Journal of the American Chemical Society 126, 3892–3901. doi:10.1021/ja039734c

Sun, Z., Xiao, Y., Agterhuis, H., Sietsma, J., Yang, Y., 2016. Recycling of metals from urban mines – a strategic evaluation. Journal of Cleaner Production 112, 2977–2987. doi:10.1016/j.jclepro.2015.10.116

Sverdrup, H.U., Ragnarsdóttir, K.V., 2014. Natural Resources in a Planetary Perspective. Geochemical Perspectives 3, 129–341. doi:10.7185/geochempersp.3.2

Tanong, K., Tran, L.-H., Mercier, G., Blais, J.-F., 2017. Recovery of Zn (II), Mn (II), Cd (II) and Ni (II) from the unsorted spent batteries using solvent extraction, electrodeposition and precipitation methods. Journal of Cleaner Production 148, 233–244. doi:10.1016/j.jclepro.2017.01.158

Thambidurai, C., Kim, Y.-G., Jayaraju, N., Venkatasamy, V., Stickney, J.L., 2009. Copper Nanofilm Formation by Electrochemical ALD. Journal of The Electrochemical Society 156, D261–D268. doi:10.1149/1.3134555

Tian, Y., Liu, H., Zhao, G., Tatsuma, T., 2006. Shape-Controlled Electrodeposition of Gold Nanostructures. The Journal of Physical Chemistry B 110, 23478–23481. doi:10.1021/jp065292q

Toraiwa, A., Abe, Y., 2000. New hydrometallurgical process of copper anode slimes at Saganoseki smelter & refinery, in: Mishra, B., Yamauchi, C. (Eds.), 2nd International Conference on Processing Materials for Properties. The Minerals, Metals & Materials Society, San Francisco, CA, United States, pp. 999–1004.

Tran, T., Davis, A., Song, J., 1992. Extraction of Gold in Halide Media, in: Misra, V.N., Halbe, D., Spottiswood, D.J. (Eds.), Extractive Metallurgy of Gold and Base Metals. The Australasian Institute of Mining and Metallurgy, Kalgoorlie, WA, Australia, pp. 323–328.

Tran, T., Lee, K., Fernando, K., 2001. Halide as an alternative lixiviant for gold processing - an update, in: Young, C.A., Tidwell, L.G., Anderson, C.G. (Eds.), Cyanide: Social, Industrial and Economic

Aspects. The Minerals, Metals & Materials Society, New Orleans, LA, United States, pp. 501–508.

Tuusjärvi, M., Mäenpää, I., Vuori, S., Eilu, P., Kihlman, S., Koskela, S., 2014. Metal mining industry in Finland – development scenarios to 2030. Journal of Cleaner Production 84, 271–280. doi:10.1016/j.jclepro.2014.03.038

Venkatraman, K., Gusley, R., Yu, L., Dordi, Y., Akolkar, R., 2016. Electrochemical Atomic Layer Deposition of Copper: A Lead-Free Process Mediated by Surface-Limited Redox Replacement of Underpotentially Deposited Zinc. Journal of The Electrochemical Society 163, D3008–D3013. doi:10.1149/2.0021612jes

Viyannalage, L.T., Vasilic, R., Dimitrov, N., 2007. Epitaxial Growth of Cu on Au(111) and Ag(111) by Surface Limited Redox Replacement – An Electrochemical and STM Study. The Journal of Physical Chemistry C 111, 4036–4041. doi:10.1021/jp067168c

Wu, Y., Fang, Q., Yi, X., Liu, G., Li, R.-W., 2017. Recovery of gold from hydrometallurgical leaching solution of electronic waste via spontaneous reduction by polyaniline. Progress in Natural Science: Materials International. doi:10.1016/j.pnsc.2017.06.009

Yliniemi, K., Wragg, D., Wilson, B.P., McMurray, H.N., Worsley, D.A., Schmuki, P., Kontturi, K., 2013. Formation of Pt/Pb nanoparticles by electrodeposition and redox replacement cycles on fluorine doped tin oxide glass. Electrochimica Acta 88, 278–286. doi:10.1016/j.electacta.2012.10.089

Zhang, G., Kuang, Y., Liu, J., Cui, Y., Chen, J., Zhou, H., 2010. Fabrication of Ag/Au bimetallic nanoparticles by UPD-redox replacement: Application in the electrochemical reduction of benzyl chloride. Electrochemistry Communications 12, 1233–1236. doi:10.1016/j.elecom.2010.06.027

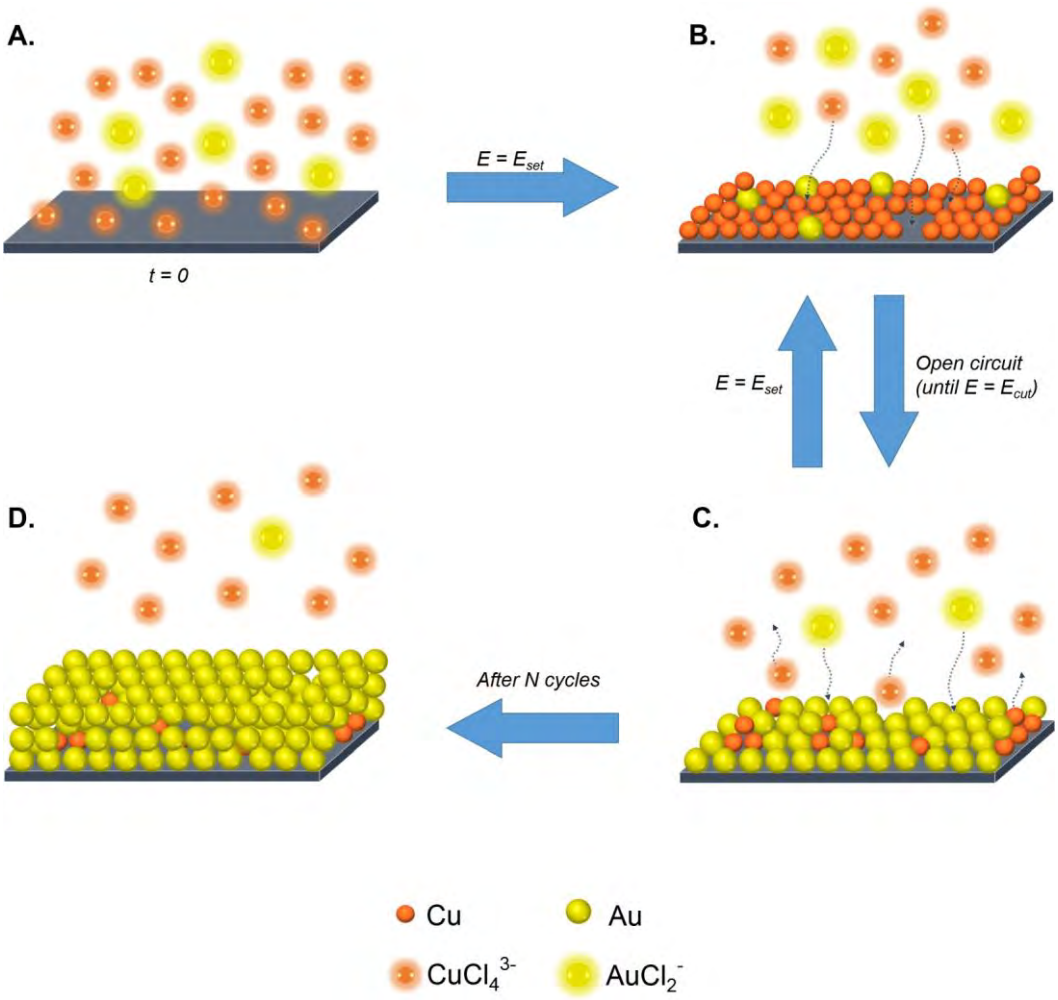

Figure 1. Mechanism of the electrodeposition-redox replacement (EDRR) in cupric chloride solution.

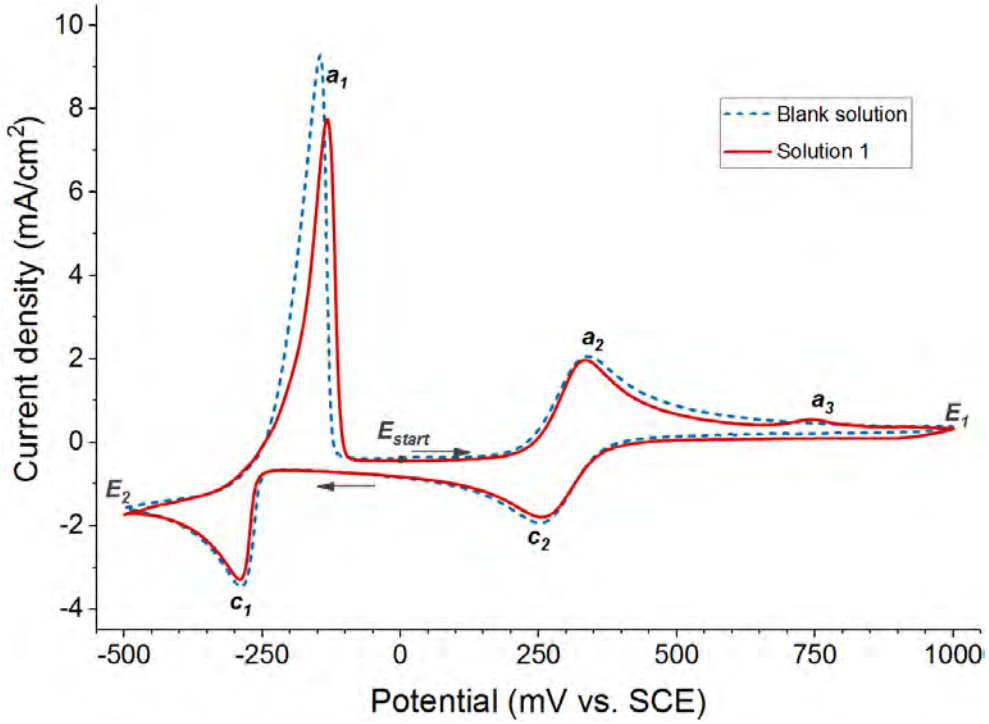

Figure 2. Cyclic voltammograms obtained from the blank solution (175 g/L NaCl and 1.2 g/L Cu) and gold-containing solution (175 g/L NaCl, 1.2 g/L Cu and 100 ppm Au): v = 50 mV/s, E_{start} = 0 mV, E_1 = 1000 mV, E_2 = –500 mV.

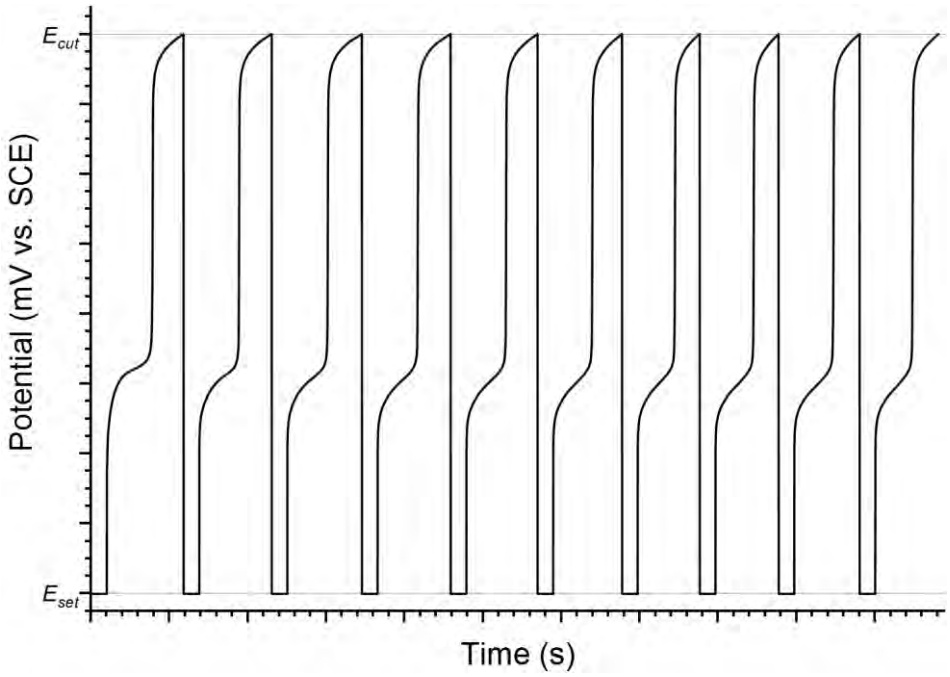

Figure 3. Typical potential vs. time curve during the EDRR process.

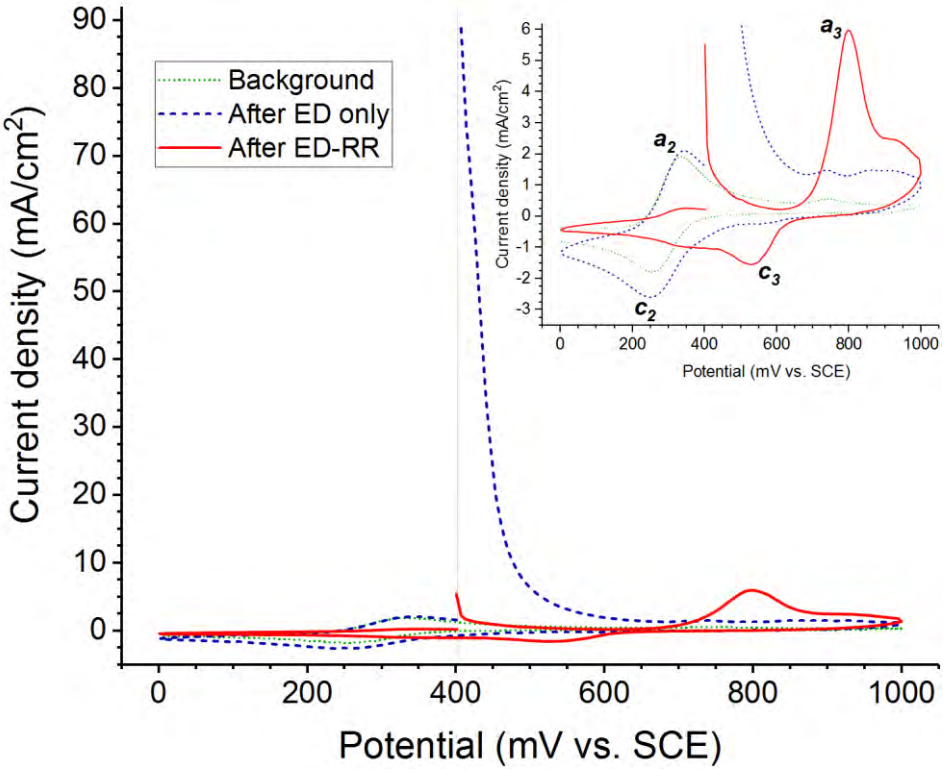

Figure 4. Cyclic voltammogram after 10 cycles of EDRR (test E11): v = 50 mV/s, E_{start} = 400 mV, E_1 = 1000 mV, E_2 = 0 mV; electrolyte – 175 g/L NaCl. Inset: magnification of the graph with a focus on the peaks observed in the experiments; ***a₂*** *– Cu^+/Cu^{2+},* ***a₃*** *– Au stripping,* ***c₃*** *– Au deposition,* ***c₂*** *– Cu^{2+}/Cu^+.*

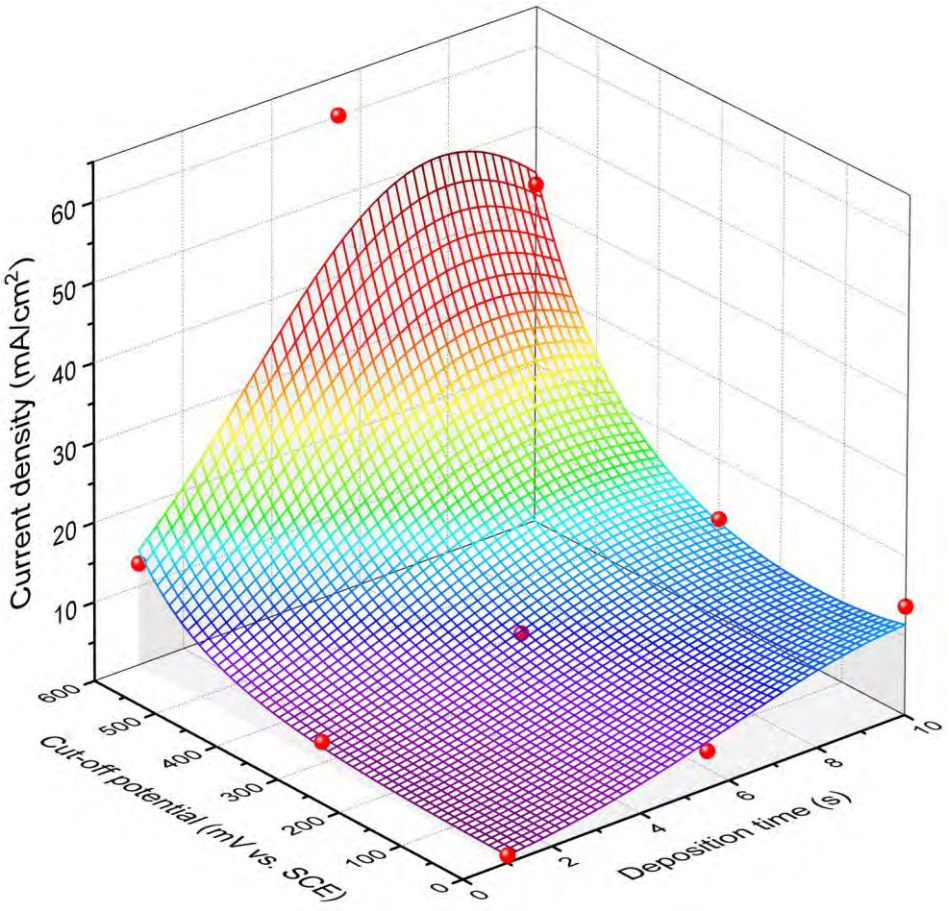

Figure 5. Response surface model and experimental data points for EDRR parameters optimization.

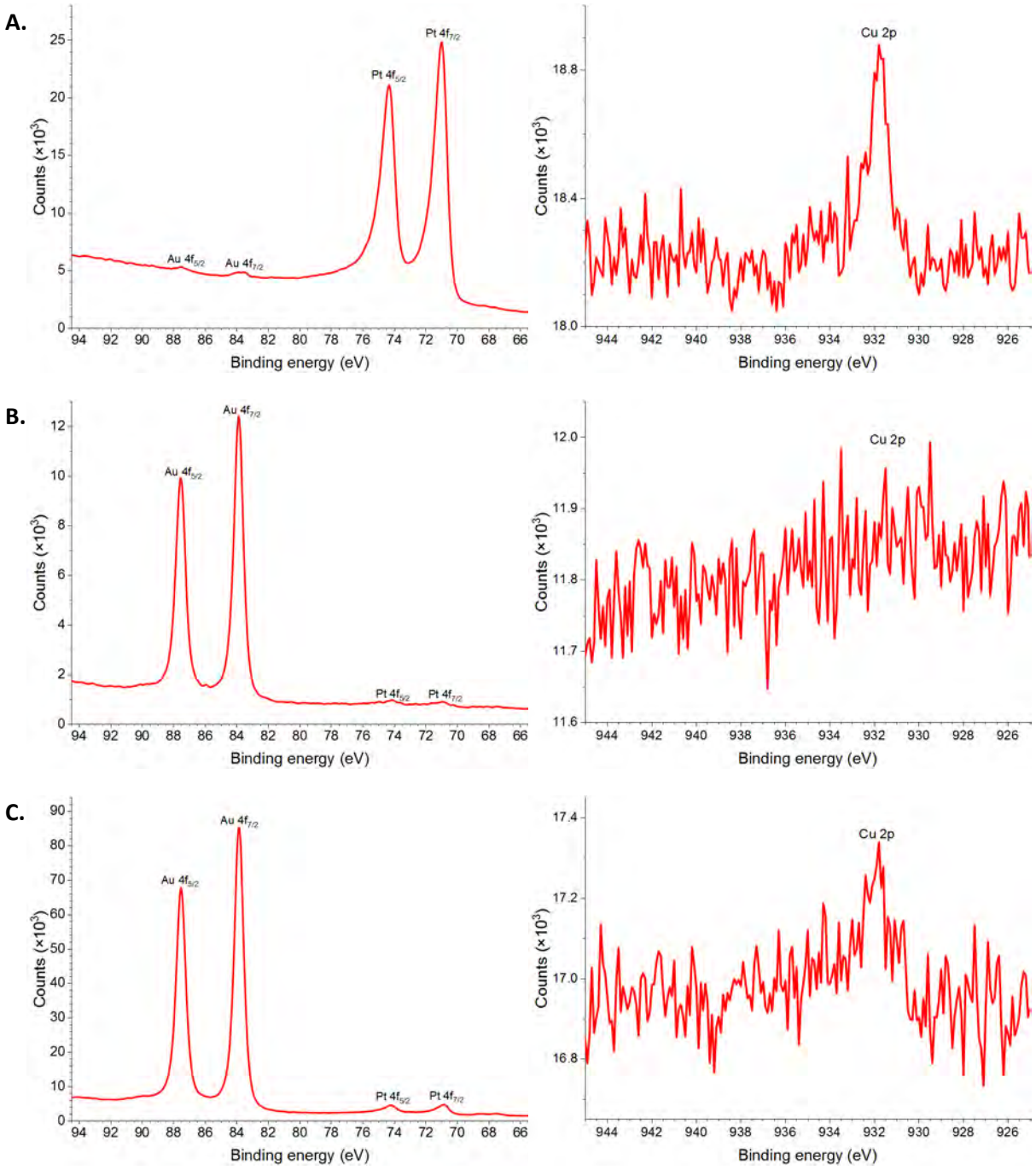

Figure 6. High-resolution XPS spectra of WE samples in Au-Pt 4f and Cu 2p regions: before test (A), after test L1 (B) and L2 (C).

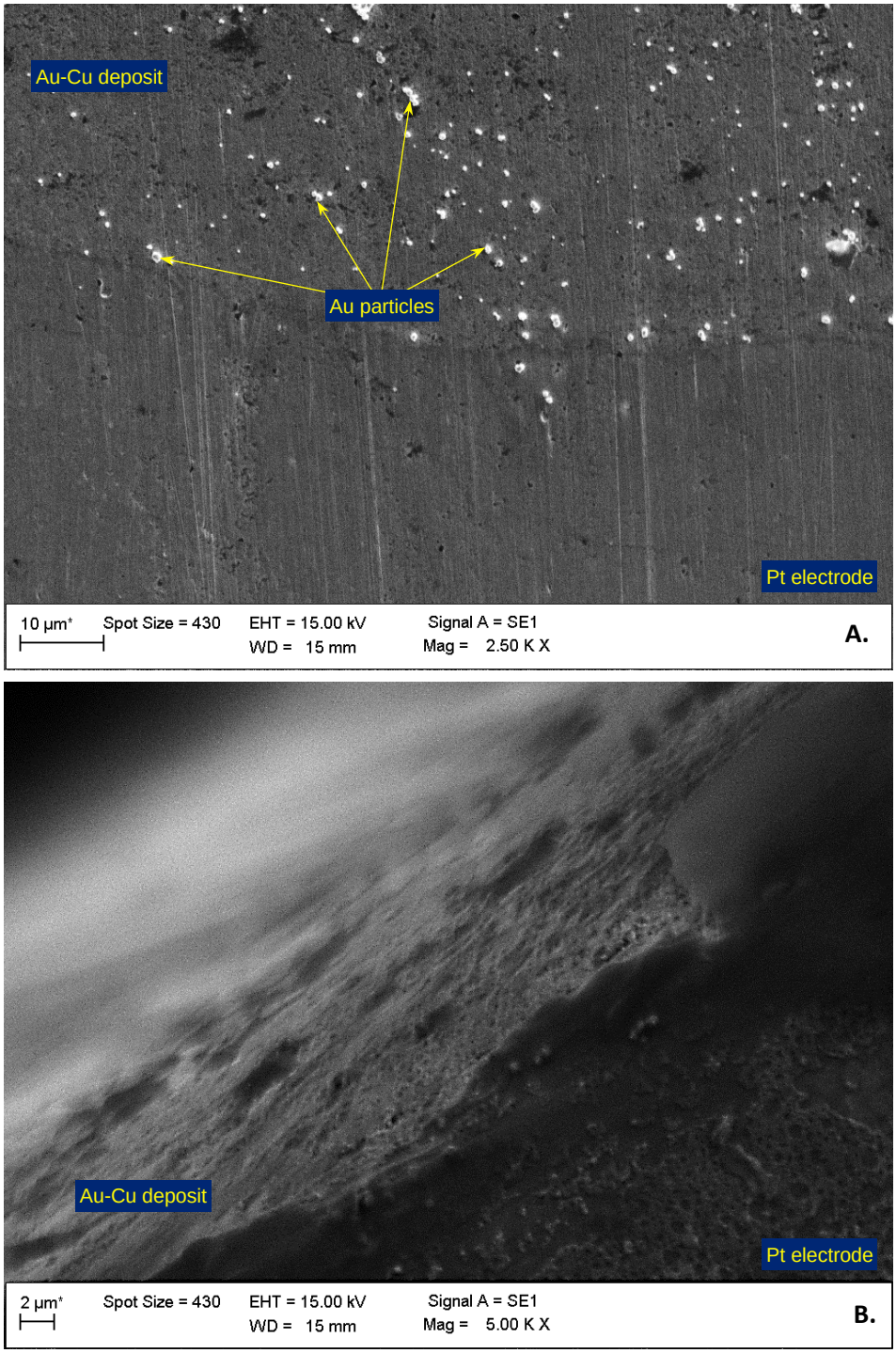

Figure 7. SEM micrographs of WE surface after EDRR (A) and its cross-section (B), test L1.

Table 1. Composition of investigated synthetic solutions.

Sample name	Composition	Au:Cu
Blank solution	175 g/L NaCl, 1.2 g/L Cu	0
Solution 1	175 g/L NaCl, 1.2 g/L Cu, 100 mg/L Au	1:12
Solution 2	175 g/L NaCl, 1.2 g/L Cu, 10 mg/L Au	1:120
Solution 3	120 g/L NaCl, 2.7 g/L Cu, 8 mg/L Au	1:340

Table 2. Investigated parameters affecting gold electrodeposition.

Test ID	[Au], mg/L	t_{dep}, s	E_{set}, mV vs. SCE	E_{cut}, mV vs. SCE	Number of cycles
E1	10	10	-500	0	10
E2	10	10	-500	300	10
E3	10	10	-300	0	10
E4	10	10	-300	300	10
E5	10	20	-500	0	10
E6	10	20	-500	300	10
E7	10	20	-300	0	10
E8	10	20	-300	300	10
E9	100	10	-500	0	10
E10	100	10	-500	300	10
E11	100	10	-300	0	10
E12	100	10	-300	300	10
E13	100	20	-500	0	10
E14	100	20	-500	300	10
E15	100	20	-300	0	10
E16	100	20	-300	300	10

Table 3. Design matrix and experimental data for optimization of gold recovery.

Test ID	t_{dep}, s	E_{set}, mV vs. SCE	E_{cut}, mV vs. SCE	Number of cycles	j_{max}, mA/cm^2
R1	1	-475	0	20	1.0
R2	1	-475	600	20	14.8
R3	1	-375	300	20	2.8
R4	1	-275	0	20	1.1
R5	1	-275	600	20	11.0
R6	5	-475	300	20	8.3
R7	5	-375	0	20	4.8
R8	5	-375	300	20	8.1
R9	5	-375	600	20	60.1
R10	5	-275	300	20	5.1
R11	10	-475	0	20	7.0
R12	10	-475	600	20	33.2
R13	10	-375	300	20	12.5
R14	10	-275	0	20	20.5
R15	10	-275	600	20	52.1
R16	5	-375	300	20	7.4
R17	5	-375	300	20	8.7

Table 4. Mass of metals recovered at the WE surface.

Test ID	Cu mass, µg/cm^2	Au mass, µg/cm^2	Au content
ED only	38.0	3.2	7.8%
EDRR (test E11)	18.2	10.8	37.2%

Table 5. Estimated effects and coefficients for j_{max} (mA/cm^2).

Factor	Effect	Coefficient	Standard error	*p*
Constant		1.4089	0.0453	0.000
Gold concentration *[Au]*	2.8477	0.0138	0.0453	0.000
Deposition time t_{dep}	0.3965	-0.0647	0.0453	0.030
Set potential E_{set}	0.1080	0.0022	0.0453	0.470
Cut-off potential E_{cut}	0.5542	-0.0074	0.0453	0.008
$[Au] \cdot t_{dep}$	0.4255	$9.5 \cdot 10^{-4}$	0.0453	0.023
$[Au] \cdot E_{set}$	0.0582	$6.5 \cdot 10^{-6}$	0.0453	0.693
$[Au] \cdot E_{cut}$	0.5631	$4.2 \cdot 10^{-5}$	0.0453	0.007
$t_{dep} \cdot E_{set}$	-0.0460	$-4.6 \cdot 10^{-5}$	0.0453	0.754
$t_{dep} \cdot E_{cut}$	0.3390	$2.3 \cdot 10^{-4}$	0.0453	0.052
$E_{set} \cdot E_{cut}$	-0.2708	$-9.0 \cdot 10^{-6}$	0.0453	0.102

Table 6. ANOVA for full factorial experimental design.

Source of variation	**DF**	**SS**	**MS**	***F***	***p***
Regression	10	37.814	3.7814	46.32	$7.04 \cdot 10^{-5}$
Residuals	6	0.4898	0.0816		
Lack of Fit (model error)	5	0.4694	0.0939	4.59	0.340
Pure error (replicate error)	1	0.0204	0.0204		
Total	16	38.304			

Coefficient of determination R^2_{adj} = 0.966

Table 7. ANOVA for the response surface model.

Source of variation	**DF**	**SS**	**MS**	***F***	***p***
Regression	5	3.7316	0.7463	36.00	$1.86 \cdot 10^{-6}$
Residuals	11	0.2281	0.0207		
Lack of Fit (model error)	9	0.2254	0.0250	18.73	0.052
Pure error (replicate error)	2	0.0027	0.0013		
Total	16	3.9597			

Coefficient of determination R^2_{adj} = 0.916

Table 8. Calculated recovery of metals from the solution at the optimized conditions.

Test ID	t_{dep}, s	E_{set}, mV vs. SCE	E_{cut}, mV vs. SCE	Number of cycles	Metal recovery		Au:Cu
					Cu	Au	
L1	5	-320	550	250	0.01%	8.4%	3.3:1
L2	10	-320	550	250	0.02%	9.3%	1.1:1